

Shape Behavior analysis of a PMN-PT [001] actuated MOEMS micro-mirror

Dragoş Adrian Ciubotariu, Cédric Clévy, Ioan Alexandru Ivan, Philippe Lutz

Abstract— This paper presents how a Lead Magnesium Niobate – Lead Titanate (PMN-PT) based actuator, poled and cut along the [001] crystalline direction, can be used as an integrated actuator in a Micro Opto Electro Mechanical System (MOEMS). This cut was chosen as it has been proved to present piezoelectric coefficients that surpass $4500\mu\text{m}/\text{V}$. This makes PMN-PT suitable for bulk usage. The actuator may be used as part of a Reconfigurable Free Space – Micro Optical Bench (RFS-MOB) to control the displacement of a micro-mirror. Finite Element simulations were used to study the influence of the actuator shape over the generated displacement, as well as the soldering medium. It was observed that for actuators with surfaces between $500\times 500\mu\text{m}^2$ and $800\times 800\mu\text{m}^2$ and a thickness of $200\mu\text{m}$, displacement of up to 370nm is achievable. While the actuator profile impacts directly on the free surface shape it is also in direct correlation with the size of the usable area of the micro-mirror.

I. INTRODUCTION

Micro-optical applications are in an ever growing demand for actuators that not only present better control but also are highly integrable. Mostly used Micro Opto Electro Mechanical System (MOEMS) are found as part of optical switches [1] [2] or optical attenuators [3] [4] but are also being used in biomedical [5] [6] imaging or astronomical applications [7]. While aiming to increase the functionality of MOEMS certain challenges emerge when dealing with localized displacement. Until recently, the preferred actuation method used either electrostatic or thermal-reactive materials such as [8] or [9] respectively. However, usage of piezoelectric actuators in MOEMS is on the rise due to improvements in piezoelectric material understanding, behavior and control. New developments target the reduction of hysteresis either through control [10] or by developing new better performing materials. Aside from having high bandwidth [11] and sub-nanometer resolution capabilities, piezoelectric actuators used in MOEMS depict interesting features, especially when actuating micro-mirrors. In order to precisely alter an optical signal micro-mirrors need to be controlled, in terms of

D.A. Ciubotariu, Cedric Clevy and Philippe Lutz are with the FEMTO-ST Institute (UMR CNRS 6174) - UFC/ENSMM/UTBM, AS2M Department, 24 Rue Alain Savary, 25000 Besancon, France (phone: +33-381-402-803; fax: +333-381-853-998; e-mail: {adrian.ciubotariu, cclevy, plutz}@femto-st.fr).

I.A. Ivan is with Université de Lyon, CNRS UMR5513, Ecole Nationale d'Ingénieurs de Saint-Etienne (ENISE), Laboratoire de Tribologie et Dynamique des Systèmes (LTDS), Université de Lyon, ENISE, LTDS UMR 5513 CNRS, 58 Rue Jean Parot, 42023 Saint-Etienne Cedex 2, FRANCE email: ivan@enise.fr.

D.A. Ciubotariu and I.A. Ivan are also with Valahia University of Targoviste, FIE/ICSTM, B-dul Unirii 18-20, 130082 Targoviste, Romania; e-mail: ivan@valahia.ro.

displacements, in the visible light spectrum: from 380 to 750nm.

Among piezoelectric materials used in MOEMS the most widely spread is Lead Zirconate Titanate (PZT), a granular structured piezoceramic material. Though widely used, it still presents drawbacks, one of which is its high hysteresis [12] that greatly impacts accuracy. More novel materials aim for better overall performances. One such material is a mono-crystalline structured piezoelectric crystal called Lead Magnesium Niobate – Lead Titanate (PMN-PT). It is a material which presents high dynamic range and piezoelectric coefficients while having reduced hysteretic behavior [13]. An advantage that stands out when using PMN-PT is the capability of it being used in bulk [14]. To this the micro-fabrication compatibility [15] is added.

In this paper bulk PMN-PT actuators are studied in order to understand their behavior when integrated in MOEMS, in particular how the PMN-PT acts as a micro-mirror actuator. This is needed as one application for the Reconfigurable Free Space – Micro Optical Bench (RFS-MOB) is micro-spectrometry. In [16] the connection between the decrease in measured displacement with the increase of the actuator width has been shown. The Finite Element simulations presented here investigate how the usable surface varies with the applied voltage for particularly shaped bulk actuators while also taking the solder into account. Experimental work has been done following the same objectives. Working domains are then defined.

The paper focuses on the use of PMN-PT as a bulk actuator for a micromirror in a RFS-MOB while investigating shape particularities and the material behavior. The direct effect of the actuator shape over the free surface displacement is noted following optical characteristics aberration limits, a tenth of the used light wavelength.

The structure that the article follows is briefly highlighted: a succinct introduction in MOEMS, the actuation principles and materials used are presented in Section I. A short description of the Reconfigurable Free Space Micro-Optical Bench (RFS-MoB) in which the studied actuator may be included is presented, along with its particularities in Section II. Section III investigates the design and simulations, while Section IV focuses on the experimental measures regarding the PMN-PT actuator. A conclusion ends the paper highlighting the results and the usable range of actuation.

II. MOEMS APPLICATION

A Reconfigurable Free Space Micro-Optical Bench (RFS-MoB) has been designed [17] using a series of purpose

oriented, removable and adjustable silicon holders. This has easy manipulation and alignment by a robotic micro-assembly station in mind. The envisioned actuator will be placed on one of the elements of the system presented in Figure.1.

Although a variety of components have already been developed, such as hybrid micro-lenses, beam splitters, micro-apertures and micro-mirrors, there is a need for enhancing the usability of the RFS-MoB. This can be done by having actuated micro-mirrors, like in the case of microspectrometry applications. This means an actuation solution needs to be adapted.

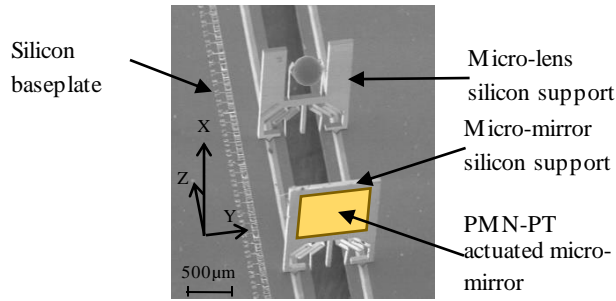


Figure 1. Assembly proposition [17].

The designed silicon micro-mirror support measures (Figure 1) $1.2 \times 0.8 \times 0.1 \text{ mm}^3$ (height x width x thickness) and presents an elastic structure at the base, for position holding in the RFS-MoB structure.

The objective of the microactuator is to fit the micro-mirror with an out-of-plane perpendicular displacement and to be integrated on the silicon support for better dynamics while maintaining a small volume (Figure 2).

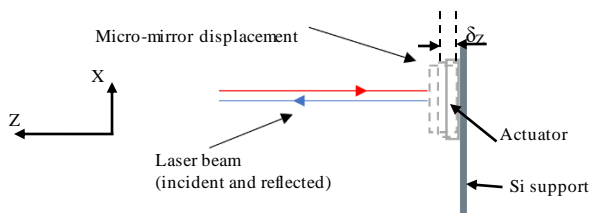


Figure 2. Actuation in respect to the vertical Si support.

The intended microactuator falls under constraints regarding surface and thickness due to the design of the silicon support: maximum usable surface of $0.8 \times 0.8 \text{ mm}^2$ (Figure 2) with a thin profile.

The displacement needed in optical applications are related to the wavelength (λ) of the light used thus a minimum is required. In the case of microspectrometry the required displacement (δz) is assumed to half the wavelength (λ) of a traditional red laser beam ($\lambda \sim 650 \text{ nm}$; $\delta z \sim 325 \text{ nm}$). To achieve this while also maintaining the thickness of the material low, materials with high and very high piezoelectric coefficients are needed. PMN-PT cut and poled along the [001] crystalline direction stands out. Recent improvements in crystal growth techniques have shown the possibility of obtaining values of over 4500 pm/V [17] for its piezoelectric coefficients. Studies on the actuation potential of PMN-PT [001] have shown that for a $200 \mu\text{m}$ thick film actuation can exceed the 325 nm limit [16].

III. FINITE ELEMENTS SIMULATIONS

Considering that the PMN-PT actuator is intended for a micro-mirror, another aspect regarding the optical necessities to be met is the maximum accepted aberration for planar displacement. This is maximum 10% of the displacement, or $\lambda/20$ in our case. The values for the FEM used parameters are gathered in Table I. Several PMN-PT [001] $200 \mu\text{m}$ thick plates were measured for their specific d_{31} and d_{33} piezoelectric coefficients using an interferometer and the average for each was used in the simulations

TABLE I. VALUES OF PMN-PT [001] SPECIFIC COEFFICIENTS

Constant	Unit	Value	Source
s_{11}^E	$\times 10^{-12} \text{ m}^2/\text{N}$	69.0	[18]
s_{12}^E		-11.1	
s_{13}^E		-55.7	
s_{33}^E		119.6	
s_{44}^E		14.6	
s_{66}^E		15.2	
d_{15}	$\times 10^{-12} \text{ C/N}$	140	measured
$d_{31}=d_{32}$		-1180	
d_{33}		2610	
$\epsilon_{11}^T/\epsilon_0$	•	1600	[18]
$\epsilon_{33}^T/\epsilon_0$		8200	

The microactuator has been simulated in COMSOL as a 3D structure fixed on one the lower side to a $30 \mu\text{m}$ thick layer that represents the solder and free on the opposite side to simulate the mirror. The underside of the solder has been fully clamped. The interface between the solder and the PMN-PT actuator have no restrictions. The solder parameters used are: a density of $\rho=7500 \text{ kg/m}^3$, Young's Modulus of $E=1.75 \times 10^{11} \text{ Pa}$ and Poisson's ration of $\nu=0.3$. Additionally, the linear shrinkage is also taken into account.

The profile of the microactuator is also important with regards to the final displacement of the microactuator free surface. As shown in [16], for a bulk square PMN-PT actuator, the corner regions show a higher displacement which slightly curve the free surface. In Figure 3 two generic, simple to manufacture profiles are presented.

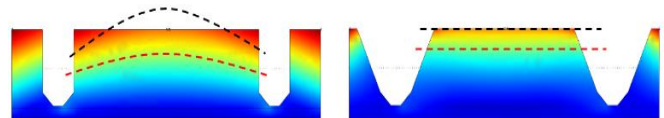


Figure 3. Same value displacement lines on two generic, different profile microactuators.

As the goal is to minimize the planar aberrations, the trapezoidal profile was chosen.

The signal applied varies between 0 V and 400 V , a value that approaches the saturation limit of PMN-PT. As displacement is sufficient, no matter the size of the actuator, the focus is on what the maximum diameter of a laser beam can be in order to stay under a maximum 10% aberration while still reaching the 325 nm displacement threshold. Figure 4 presents a schematic view of the important parameters: the

displacement δ_z , the aberration limit $\lambda/20$, the width of the microactuator w and the maximum diameter of the usable surface Φ_{\max} .

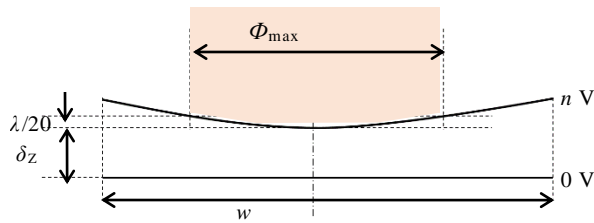


Figure 4. Microactuator free surface shape and variables of interest for an applied voltage of nV .

Following the schematic presented in Figure 5, simulations were done on several PMN-PT microactuators, with the corresponding values presented in Table II. The base width of the microactuator, at the edge of the blade is W , w is the free surface width, h is the PMN-PT microactuator thickness, h_0 is the depth of the separating groove and h_p is the silver solder thickness. Since the FEM simulations provide linear behavior, the applied voltage was equal to the maximum voltage used in the experiments.

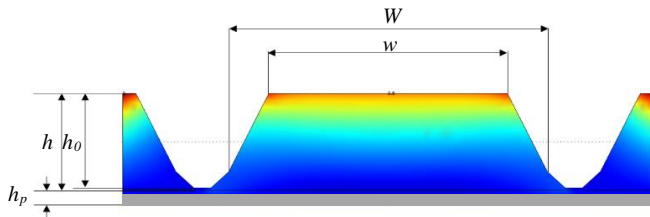


Figure 5. Profile of a simulated PMN-PT microactuator.

The values for h_0 and w have been measured using a Polytec® MSA-500 MEMS analyzer.

TABLE II. PMN-PT [001] DIMENSION SPECIFIC PARAMETERS USED FEM SIMULATIONS

W (μm)	w (μm)	h (μm)	h_0 (μm)	h_p (μm)
300	192	200	190	30
400	295	-/-	191	-/-
500	391	-/-	187	-/-
600	497	-/-	188	-/-
700	593	-/-	194	-/-
800	680	-/-	192	-/-

The solder layer also presents an influence over the microactuator free surface displacement. A direct comparison between a rigid solder (Gold on Gold) and an elastic silver based epoxy shows not only a doubling of the displacement in the central region but also a 10% decrease for the outer corners, as shown in Figure 6. This has to do more with the mechanical characteristics of the adhesive film, rather than its thickness.

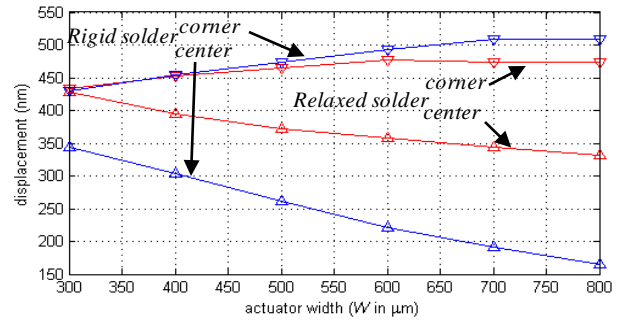


Figure 6. FEM simulations comparison between a Rigid (similar to Gold-on-Gold) solder and an Elastic (Silver-Epoxy) solder.

One major positive effect of this style of actuator fixing is that the solder linear contraction induced by its curing is in the same direction as the actuator planar displacement during actuation. This is due to the PMN-PT [001] negative d_{31} and d_{32} piezoelectric coefficients (Table I).

IV. EXPERIMENTS WITH PMN-PT

The microactuators studied in this paper have been manufactured following a process that is succinctly presented as follows.

Several gold-plated PMN-PT [001] samples, measuring $3 \times 3 \times 0.2 \text{ mm}^3$ were cut from a $20 \times 20 \times 0.2 \text{ mm}^3$ TRS Technologies® fabricated plate. They were then soldered onto glass plates using EPO-TEK® 22H, a conductive, silver based solder measuring $30 \mu\text{m}$ in thickness. Each plate was then cut using a saw dicing machine in order to obtain individual microactuators measuring from $500 \mu\text{m}$ to $800 \mu\text{m}$ in width. Gold wires measuring $25 \mu\text{m}$ in diameter were connected using the ball-edge wire bonding technique.

A poling procedure then followed, in order to eliminate any fabrication induced losses. $400V$ were applied to the bulk PMN-PT microactuators while placed in an oven that was then heated up to 200°C in 60 minutes, kept there for 30 minutes and then allowed to cool down to room temperature for 90-120 minutes before reducing the voltage to zero. Displacement results after repoling are exemplified in Figure 8.

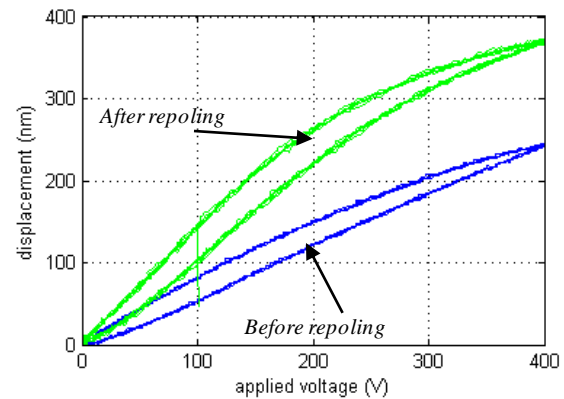


Figure 7. Displacement found experimentally on a $700 \times 700 \mu\text{m}^2$ PMN-PT bulk microactuator before and after high temperature repoling. A 53% increase is noticed.

The experiments were conducted using the stand schematically presented in Figures 8 and partially shown in Figure 9.

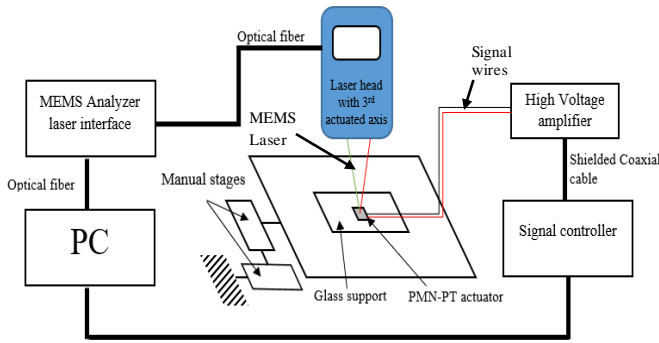


Figure 8. Schematic of the experimental stand used for the PMN-PT microactuator displacement measurements.

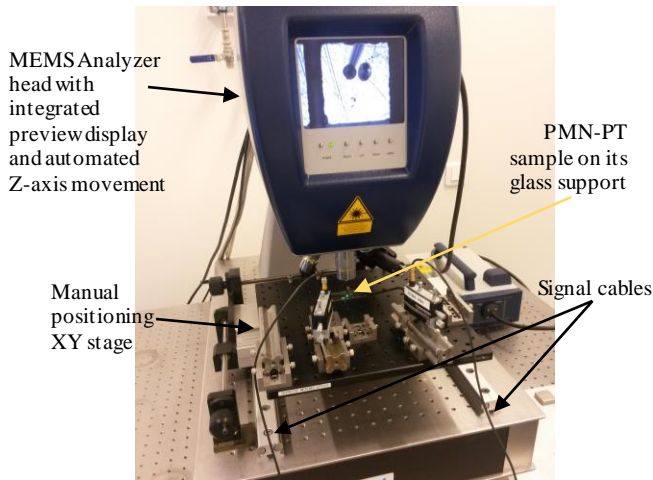


Figure 9. MEMS Analyzer laser head and positioning stages with a close up view of the actuator on the available display

The sample was positioned under the laser beam of the MEMS Analyzer on a precision, manually actuated, in-plane positioning stage onto which the signal wires were also fixed. The fine calibration and focusing of the measuring laser beam is done automatically with the aid of a piezoelectric stack situated inside the MEMS Analyzer head. A sine waveform with a peak-to-peak amplitude of 400V and a frequency $f=3\text{Hz}$ was applied on the positive front using a high voltage amplifier. The MEMS Analyzer interferometry function was used in order to measure the displacement of points on the free surface of the actuator. A matrix of 7×7 points was overlaid on the microactuator, as exemplified in Figure 10. The passage from point to point was done automatically followed by a manual reselection of the initial measured point, for cross-reference. Measurements were made on PMN-PT actuators having widths of $500\mu\text{m}$, $600\mu\text{m}$, $700\mu\text{m}$ and $800\mu\text{m}$.

The displacement measured for each of the sizes is compared with its corresponding model in Figure 11.

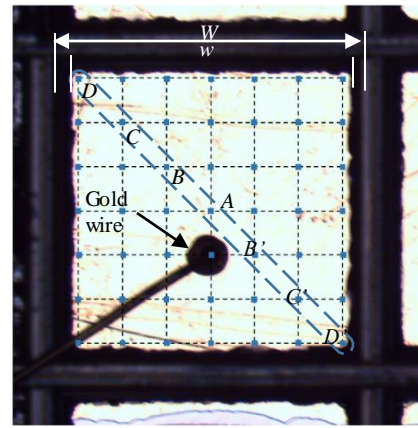


Figure 10. Top view of an $800 \times 800 \mu\text{m}^2$ PMN-PT microactuator with the superimposed guidance matrix for the Measuring Laser beam of the MEMS Analyzer.

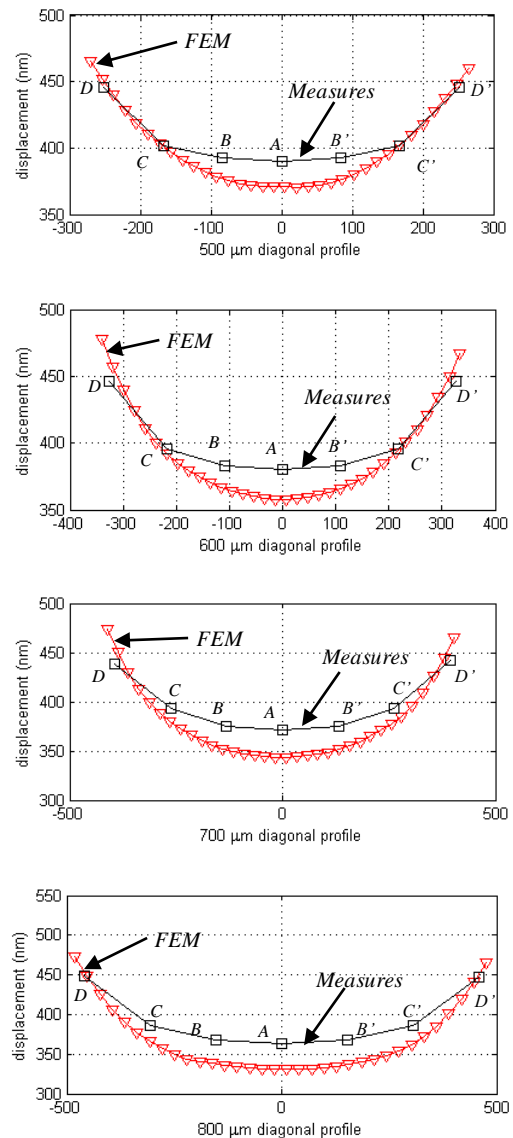


Figure 11. Comparison between FEM simulations and experimental results for (top to bottom) the $500\mu\text{m}$, $600\mu\text{m}$, $700\mu\text{m}$ and $800\mu\text{m}$ wide actuators (highlighted points correspond to those mentioned in Figure 10).

The measurements indicate that the wire bonding does not have a noticeable effect on the final shape of the PMN-PT actuator or of the overall displacement.

Figure 12 brings together the minimum and maximum displacements for the different size microactuators. It is noticed that the difference surpasses the maximum aberration limit imposed by a microspectrometry application of $\lambda/20$ ($\sim 32.5\text{nm}$).

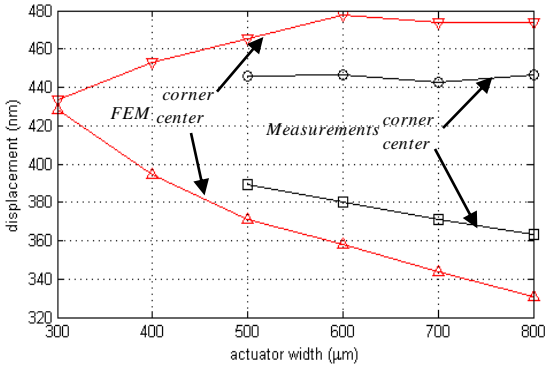


Figure 12. Comparison between the FEM simulations and the Silver-Epoxy soldered actuators experimental results.

Of the two conditions the micro actuator needs to fulfill, the minimum displacement is achieved at different voltages, depending on the width of the actuator (Figure 13). These voltages also represent the minimum values that need to be applied in order to fulfill the second condition, the desired displacement (for each actuator width) of $\lambda/2$. As mentioned previously (Figure 5), there is a maximum laser beam diameter that can be used to remain under the $\lambda/20$ aberration limit. While measurements show a more reduced curvature of the free surface than the FEM simulation, the difference between the center and the outer corners still surpasses the imposed limit. The variation of the laser beam diameter is presented in Figure 14, while taking into account the minimum required voltages.

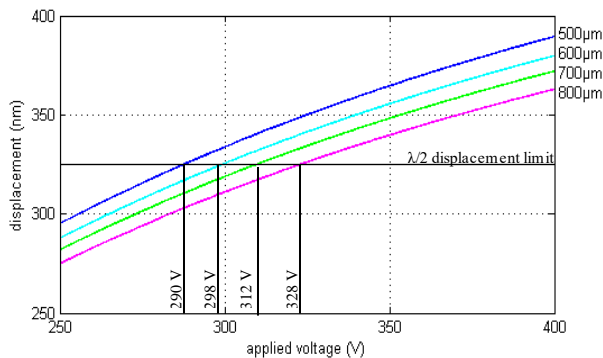


Figure 13. Close view of the different voltage values where minimum actuation is achievable, depending on the microactuator width.

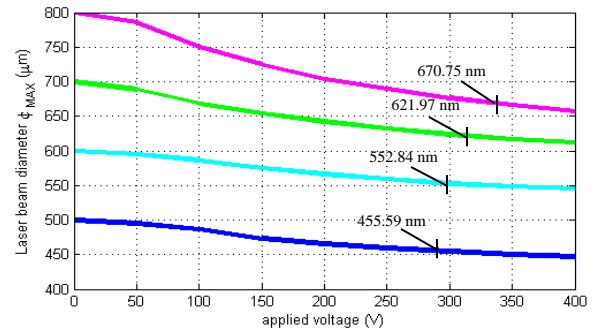


Figure 14. Laser beam maximum diameter (Φ_{MAX}) variation with applied voltage.

The points highlighted in Figure 14 represent the maximum laser beam diameter (Φ_{MAX}) values usable for the minimum applied voltage in order to reach $\lambda/2$ displacement.

The results lead to the following conclusions: first, the minimum desired displacement can be achieved with large size microactuators ($800 \times 800 \mu\text{m}^2$), making fabrication easier and allowing for larger diameter beams to be used and second, the free face large displacement allows for a wider range of color lasers to be used.

V. CONCLUSION

The paper has presented the design, modeling and characterization of a bulk $200 \mu\text{m}$ thick PMN-PT actuator poled in [001] crystalline direction. PMN-PT [001] can be used for a MOEMS micro-mirror actuator and, in this paper, its behavior was captured through FEM simulations and validated through experimental measurements. A contribution of the paper is the influence the solder brings to the free surface movement. It was observed that a minimum $\lambda/2$ displacement, when $\lambda=650\text{nm}$, can be achieved with bulk trapezoidal profile shaped actuators, $800 \mu\text{m}$ wide at the base, with voltages under 340V or as low as 290V for actuators measuring $500 \mu\text{m}$ at the base. These values are unobtainable with classic PZT ceramics used in bulk. The influence of the clamping interface on the displacement of large microactuators is also taken into account. Another contribution is the definition of the laser beam maximum usable diameter (Φ_{MAX}) in regards to the size of the actuator, while achieving a minimum 325nm required actuation.

The main advantage of PMN-PT [001], when used as an integrated actuator, is the possibility of it being used in bulk as the sub-millimeter dimensions of the support do not allow for piezostack type actuators. To this, the simplicity of fabrication with standard techniques is added, achieving similar displacements for lower voltages.

ACKNOWLEDGMENT

These works were partly supported under the Franche-Comte REGION and UEFISCDI PN-II-RU-TE-2011-3-0299 (ADMAN). We acknowledge the Labex ACTION project (ANR-11-LABX-01-01) and the French RENATECH network through its FEMTO-ST technological facility and the technical support of Vincent Chalvet.

REFERENCES

- [1] Y. Lv, Q. Feng, L. Liu, Q. Yi and Y. Li, "Application of optical switch in precision measurement system based on multi-collimated beams", *Measurements*, Vol. 61, pp. 216-220 (2015)

- [2] C. Tsai and J. Tsai “MEMS optical switches and interconnects”, *Displays*, In press (2014)
- [3] Q. Wu, L. Zhou, X. Sun, H. Zhu, L. Lu and J. Chen “Silicon thermo-optic variable optical attenuators based on Mach–Zehnder interference structures”, *Optics Communications*, Vol. 341, pp. 69-73 (2015)
- [4] HuaJuan Qi et al “The thermo-optical variable optical attenuator based on SOI”, *Optik*, Vol. 125, Issue 2, pp. 6987-6990 (2014)
- [5] R. Guldiken and O. Onen “MEMS ultrasonic transducers for biomedical applications”, *Mems for Biomedical Applications*, pp. 120-149 (2012)
- [6] Lin Liu et al. “MEMS-based 3D confocal scanning microendoscope using MEMS scanners for both lateral and axial scan”, *Sensors and Actuators A: Physical*, Vol. 215, pp. 89-95 (2014)
- [7] H. Song, R. Fraanje, G. Schitter, G. Vdovin and M. Verhaegen “Controller Design for a High-Sampling-Rate Closed-Loop Adaptive Optics System with Piezo-Driven Deformable Mirror”, *European Journal of Control*, Vol. 17, Issue 3, pp. 29-301 (2011)
- [8] S. Hourri, D. Aubry, P. Gaucher and E. Lefeuvre “An electrostatic MEMS frequency up-converter for efficient energy harvesting”, *Procedia Engineering*, Vol. 87, pp.1222-1225 (2014)
- [9] J.C. Chiou, L.C. Chou, Y.L. Lai and S.C. Huang “A novel thermal switch and variable capacitance implement by CMOSMEMS process approaching in micro electrostatic converter”, *Solid-State Electronics*, Vol. 77, pp. 56-63 (2012)
- [10] X. Wang, V. Pommier-Budinger, A. Reysset and Y. Gourinat “Simultaneous compensation of hysteresis and creep in a single piezoelectric actuator by open-loop control for quasi-static space active optics applications”, *Control Engineering Practice*, Vol. 33, pp. 48-62 (2014)
- [11] P.C. Hunag, T.H. Tsai and Y.J. Yang “Wide-bandwidth piezoelectric energy harvester integrated with parylene-C beam structures”, *Microelectronic Engineering*, Vol. 111, pp.214-219 (2013)
- [12] N. Wongdamnern et al. “Comparative studies of dynamic hysteresis responses in hard and soft PZT ceramics” *Ceramics International*, Vol. 34 pp.731-734 (2008)
- [13] A. Chaipanich et al. “Dielectric and ferroelectric hysteresis properties of 1–3 lead magnesium niobate–lead titanate ceramic/Portland cement composites”, *Ceramics International*, Vol.38S,pp.S255-S258 (2012)
- [14] Gang Tang et al. “Development of high performance piezoelectric d_{33} mode MEMS vibration energy harvester based on PMN-PT single crystal thick film”, *Sensors and Actuators A: Physical*, Vol: 205, pp.150-155 (2014)
- [15] I. A. Ivan, J. Agnus and P. Lambert “PMN–PT (lead magnesium niobate–lead titanate) piezoelectric material micromachining by excimer laser ablation and dry etching (DRIE)” *Sensors and Actuators A: Physical*, Vol. 177 pp.37-47 (2012)
- [16] D. A. Ciuboariu, I. A. Ivan, C. Clévy and P. Lutz “Size-dependent Analysis and Experiments of Bulk PMN-PT [001] Piezoelectric Actuator for MOEMS Micro-Mirrors”, *Advanced Intelligent Mechatronics (AIM) IEEE*, (2014)
- [17] S. Bargiel, K. Rabenorosa, C. Clévy, C. Gorecki and P. Lutz “Towards micro-assembly of hybrid MOEMS components on a reconfigurable silicon free-space micro-optical bench”, *Journal of Micromechanics and Microengineering*, Vol; 20, Issue 4 (2010)
- [18] N.Yamamoto, Y.Yamashita, Y.Hosono, K.Itsumi “Electrical and physical properties of reepoled PMN–PT single-crystal sliver transducer”, *Sensors and Actuators A: Physical*, vol.200 pp16-20 (2013)